Proc. Indian Acad. Sci. (Earth Planet. Sci.), Vol. 99, No. 4, December 1990, pp. 693–716.

Magnetometer array studies in India: Present status, data interpretation and assessment of numerical modelling results

B R ARORA

Indian Institute of Geomagnetism, Colaba, Bombay 400 005, India

Abstract. Significant results from several array of magnetometers deployed in India to probe deep geoelectrical structures of the crust and the upper mantle are reviewed in this paper. Emphasis is on critical appraisal of earlier results so that the article summarizes what has been done so far and what caution is to be taken on future work.

Two large-scale arrays over northwest and peninsular India during 1979–80, have been followed up with six more linear or two-dimensional arrays over different parts of the country. "Trans-Himalayan" conductor aligned along the strike of Aravalli range, delineated by arrays over northwest India, essentially represents one of the major continental induction anomalies mapped by electromagnetic methods. Efforts for quantifying the induction effects through numerical models are shown to be constrained due to the large inter-station spacing, lack of information on the regional background conductivity distribution and the non-inclusion of the frequency dependence of induction effects. A more comprehensive modelling, not biased by these factors, enables approximating the Trans-Himalayan conductor as an asymmetric domal upwarp in the middle and lower crust located between Delhi-Hardwar ridge and Moradabad fault. Numerical modelling results for southern peninsular, despite the constraints, indicate that the strong and complex induction pattern can be adequately attributed to the combination of conductors connected with triple junction between Indo-Ceylon Graben, Comorin ridge and the west coast rifting.

Induction features derived from the Valsad array, operated over basalt-covered region of western India, demarcate an enhanced conducting zone beneath Plume-associated triple junction in the Gulf of Cambay, apart from characterizing the presently active seismic zone as a resistive block.

Keywords. Electromagnetic methods; magnetometer array studies; geoelectrical structures; transient geomagnetic variations; conductivity anomalies; geomagnetic depth sounding.

1. Introduction

Magnetometer arrays are deployed to investigate the electrical conductivity structure of the earth's crust and the upper mantle. Electrical conductivity distribution thus derived serves as a window to look into the earth's interior and possibly throw light on the geological processes. The parametrization of the earth in terms of electrical conductivity has its significance owing to its dependence on the chemical composition and thermal state, association with low velocity zone and partial melting, correlation with stress changes and a possible precursor for earthquake studies. Over the last two decades, magnetometer array studies (MAS) have been increasingly used for probing and mapping conductive structures in a variety of geological environments such as sedimentary basins, ancient platforms and crystalline shields, orogenic belts, rift zones etc. Some important findings from MAS have been reviewed in Hutton (1976), Adam (1980), Singh (1980), Alabi (1983), Gough (1983) and Hjelt (1988).

In India, systematic MAS commenced in 1979 as a collaborative exercise between the Indian Institute of Geomagnetism (IIG), the National Geophysical Research Institute (NGRI) and the Australian National University (ANU). Under this joint scheme, two arrays using the ANU set of Gough-Reitzel magnetometers were carried out over the northwest and peninsular India. Following this a set of Gough-Reitzel magnetometers has been indigenously fabricated at IIG. Under the various projects sponsored by the Department of Science and Technology (DST), Government of India, some six linear or two-dimensional arrays have also been carried out by IIG over different parts of the country. The geographical locations of these arrays on the map of India are shown in figure 1. This paper is an attempt to review the notable results of some of these arrays. The results of the Garhwal and the Kangra array are discussed in some detail to illustrate the state-of-art of the widely used interpretational techniques to deduce the flow path of internal induced currents and associated conductive structures from transient geomagnetic variations. Towards the end of the section on these interpretational techniques, a reference is made to the method adopted for numerical modelling of the mapped structures. Giving the main anomalous features of data, we will focus our attention on the quantification of the results from the NW India and Peninsular India.

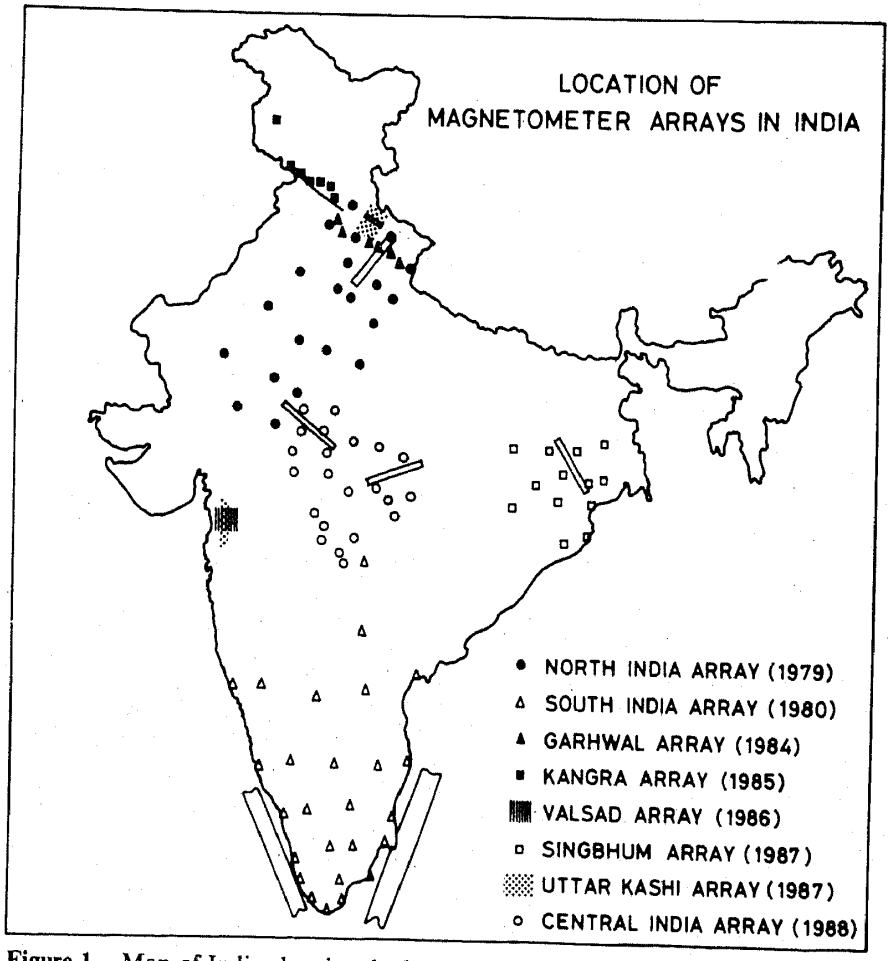

Figure 1. Map of India showing the locations of magnetometer arrays, operated between 1979–1988, together with the position of mapped conductive structures.

The results of the Valsad array are presented to demonstrate the efficacy of the electromagnetic method in delineating the sub-surface structures beneath the basalt-covered region. The arrays over Central India and Singhbhum are designed to provide information on the structural setting of Narmada-Tapti lineament and Singhbhum botholith respectively; the data of these arrays are at different stages of analysis and are therefore not considered here.

2. Data and interpretation

The physical entities measured by a magnetometer array are the time-varying magnetic field in the vertical component (Z, positive downward) and in two horizontal components (X, northward positive, and Y, eastward positive, or the components H and D in the local magnetic northward and westward coordinates at each station). Some idea on the nature of lateral conductivity distribution in the area under investigation can be obtained by the examination of stacked magnetograms of selected disturbance events in time domain. As induction process is frequency-dependent much of the analysis of the array data is carried out in the frequency domain. Several techniques have been developed for analysis, presentation and interpretation of the array data.

2.1 *Maps of Fourier transform parameters*

When data from large 2-D magnetometer array are available, the contoured maps corresponding to Fourier amplitude and phase (or cosine and sine transform) at selected frequencies of magnetovarional events prove useful in locating anomalous concentrations of internal induced currents (Reitzel *et al* 1970; Gough and Ingham 1983). In an application of this technique on the NW Indian array data, Lilley *et al* (1981) introduced one additional map corresponding to the total strength of the horizontal field, obtained by combining the amplitude of X and Y components, which were helpful in tracing the local perturbation in the flow path of regional induced currents. This method also proved useful in delineating some shallow conductive zones related with sediment-filled troughs at the Ganga basin (Arora *et al* 1982).

2.2 *Transfer functions*

A more quantitative estimation of a sub-surface structure requires separation of recorded fields (F) into normal (F_n) and anomalous (F_a) parts, distinct from the separation into external and internal parts (Schmucker 1970). The normal part is the vector sum of the external field and its electromagnetic response in layered, usually one-dimensional, earth model for the region. The anomalous part exists only if the medium has lateral inhomogeneities of conductivity. Schmucker (1970), describing the formal theoretical approach, showed that a useful measure of the inductive response of the earth is given by a set of transfer functions obtained by relating the anomalous field components with normal field components. He showed that under the quasiuniform nature of the external inducing field, when the normal part of the vertical field (Z_n) tends to be negligible, the relationship between the Fourier transform

of the anomalous and normal field can be expressed as

$$X_a = T_{xx} \cdot X_n + T_{xy} \cdot Y_n + \varepsilon_x, \tag{1}$$

$$Y_a = T_{yx} \cdot X_n + T_{yy} \cdot Y_n + \varepsilon_y, \tag{2}$$

$$Z_a = T_{zx} \cdot X_n + T_{zy} \cdot Y_n + \varepsilon_z, \tag{3}$$

where all quantities are complex and frequency-dependent. The subscript a and n refer to the anomalous and normal parts of the respective field components. ε denotes the uncorrelated part which may account for the field of external origin. With simultaneous records from an array of stations, there are various methods of choosing the X_n and Y_n to combine with the anomalous parts of any particular station (e.g. see Gough and de Beer 1980). The complete description of the underlying assumptions and the practical care to be adopted towards stable estimation of the transfer functions are given in Beamish (1977) and Gough and Ingham (1983). Ideally the transfer functions, set of T's, so derived contain the required information concerning the nature of internal field and thus characterize the anomalous conductivity structure in the vicinity of measuring site. For ease of graphical presentation and physical interpretation, Schmucker (1970) introduced two set of arrows, induction and perturbation arrows, as defined below.

2.3 *Induction arrows*

Let $\mathbf{i}$ and $\mathbf{j}$ be the Cartesian unit vectors pointing towards north (x) and east (y) respectively and the induction arrows for one particular frequency are defined as

Real induction arrow

$$I_{\text{real}} = \text{Re}[T_{zx}] \cdot \mathbf{i} + \text{Re}[T_{zy}] \cdot \mathbf{j}. \tag{4}$$

Quadrature induction arrow

$$I_{\text{imag}} = \text{Im}[T_{zx}] \cdot \mathbf{i} + \text{Im}[T_{zy}] \cdot \mathbf{j}. \tag{5}$$

It is usual to reverse the direction of the real arrows so that they point at right-angles towards the region of high internal electrical conductivity. Such a property of induction arrows, when displayed on the map of stations grid, clearly identifies the location and strike of sub-surface anomalies. Their magnitude, spatial distribution pattern and frequency-dependent contains information on the depth and lateral extent of the involved conductive structure. An example of the mode of presentation of the induction arrow appears in figure 3.

2.4 *Perturbation arrows*

Complex perturbation arrows $\mathbf{p}$ and $\mathbf{q}$ are formed by combining the horizontal transfer functions (T_{xx}, T_{xy}, T_{yx}, T_{yy}) such that

$$\mathbf{p} = -T_{xx} \cdot \mathbf{i} - T_{yx} \cdot \mathbf{j} \text{ and} \tag{6}$$

$$\mathbf{q} = T_{xy} \cdot \mathbf{i} + T_{yy} \cdot \mathbf{j} \tag{7}$$

for both real and quadrature arrows. With respect to the definition by Schmucker (1970), the sign of **p** arrows has been reversed and for their interpretation and pictorial presentation, both **p** and **q** are rotated 90° clockwise so that they directly represent the strength and direction of the anomalous internal current field which are superimposed on the unperturbed normal current flow along the east and north respectively. Further, when both **p** and **q** are added vectorially, the resultant **p** + **q** arrows describe the overall flow pattern of the anomalous induced currents. The perturbation arrows are more effective in detecting distinct conductors which might exist near each other (Arora 1987). Another example of the efficacy of perturbation arrows in tracing the flow path of anomalous internal currents is discussed in the section on the results of the Valsad array.

2.5 *Anomalous induction arrows*

More recently, Jones (1983, 1986) introduced yet another set of arrows, termed anomalous induction arrows which he considered were a more useful response function in locating the anomalous conducting zones than the conventional induction arrows. The anomalous induction arrows are derived from a set of transfer functions relating the anomalous part of the variations in the three components at any given site, viz:

$$Z_i - Z_n = T'_{zx}\cdot(X_i - X_n) + T'_{zy}\cdot(Y_i - Y_n) + \varepsilon. \tag{8}$$

The usefulness of these arrows is tested in a complex region of District Valsad where the nature of induction effects appears to be determined by more than one conductor.

2.6 *Hypothetical event analysis (HEA)*

Given the set of transfer functions evaluated from the observed data, the process can be reversed and by appropriately choosing the X_n and Y_n in equations (1)–(3), the anomalous vertical and horizontal field that would be associated with a normal field of given strength and polarization can be computed. For example, the real and imaginary parts of the anomalous vertical field resulting from a normal field-of-unit amplitude and making an angle θ with respect to north can be calculated as follows:

$$Z_R = \mathrm{Re}(T_{zx})\cos\theta + \mathrm{Re}(T_{zy})\sin\theta, \tag{9}$$

$$Z_I = \mathrm{Im}(T_{zx})\cos\theta + \mathrm{Im}(T_{zy})\sin\theta. \tag{10}$$

The real and imaginary parts of the predicted anomalous response can be further combined to estimate the modulus and the phase of the anomalous field:

$$Z_M = (Z_R^2 + Z_I^2)^{\frac{1}{2}}; \tag{11}$$

$$Z_\phi = \tan^{-1}[Z_I/Z_R]. \tag{12}$$

Estimating the anomalous field response through this method was first suggested by Bailey *et al* (1974) and the method is termed the hypothetical event analysis (HEA). The technique can be effectively used to map the polarization dependence of anomalous field, which facilitates inference on the strike and dimensionality of the mapped conductive structure. Two complimentary modes of the presentation of the array data using this techinque will appear in this paper.

Arora (1987) used this technique to simulate maps of anomalous fields for the NW India array. Board agreement of these maps with directly observed Fourier transform maps provided experimental support to the hypothesis of Beamish (1977) that HEA could be construed as being an equivalent method of presentation to maps of Fourier-transform parameters.

2.7 *Numerical modelling techniques*

Once the anomalous features of the conductor are identified, its depth, geometry and conductivity contrast can be obtained by recourse to numerical modelling. Different 2-D and 3-D numerical modelling techniques have been developed over the last two decades. The complete details of this techinque are beyond the scope of this paper and the reader is requested to refer to Kaikkonen (1986) for the present status of numerical modelling techniques. The approach has often been that of forward modelling. In this procedure, after defining the model and its parameters, the response function is computed and compared with the observed one. The parameters of the model are then changed until a satisfactory fit is obtained between computed and observed responses. The numerical response of 2-D or 3-D structures can be carried out by the methods in which the techniques of either differential equation or integral equations are used. The solution of differential equations is obtained using either the finite difference or the finite element approximations. The 2-D numerical modelling programs developed by Jones and Pascoe (1971) and Brewitt-Taylor and Weaver (1976) are now widely used. Both these techniques allow use of complicated shapes and different conductivity contrast to stimulate mapped conductor. Chamalaun *et al* (1987) and Arora and Mahashabde (1987) modelled the Trans-Himalayan conductor using the formulation of Jones and Pascoe (1971), whereas Arora *et al* (1991) used the scheme of Brewitt-Taylor and Weaver (1976). The application of 3-D modelling technique to account for complete electromagnetic effects around the Indian Peninsula and the Sri Lankan island has been developed by Ramaswamy *et al* (1985). This method is expensive in terms of computer time and storage, and only simple geometries were tried. In an alternative approach to simulate 3-D structures of the southern India, thin-sheet approximation technique has been applied by Mareschal *et al* (1987). In this technique, the anomalous structure is represented as a thin sheet of variable conductance at the surface of a layered earth. This technique has proved effective and a useful way to consider the electromagnetic distortion effects due to near surface inhomogeneities or current channelling.

3. Geomagnetic induction anomalies in northwest India

Lilley *et al* (1981) and Arora *et al* (1982) have given a detailed account of the magnetometer array study in the NW India. While in the former, a path of concentrated current flowing in the earth striking across the Himalaya was delineated, in the latter a variety of conductive structures have been mapped in the area. Arora *et al* (1982) noted that the major conductive structure, following the strike of the Aravalli mountain belt of Indian Shield, appears to run across the Ganga basin into the foothills of Himalaya. Being aligned transverse to the Himalayan mountains, the conductive structure has been named "Trans-Himalayan" conductor (Arora 1988).

Away from the influence of this massive structure, results from this array indicated, amongst others, the presence of a relatively shallow electrical discontinuity along the foothills of Himalaya. It is a matter of critical appraisal whether one should restrict the area and pick up better response or cover large area and revisit the area to decipher the anomaly with closer spacings along the profiles of interest. The Garhwal and the Kangra arrays were primarily designed to supplement further data on the two structures delineated through the 1979 NW India array. Location of magnetometer sites covered during these linear arrays is shown in figure 2 together with the principal tectonic features of the region. Also shown in figure 2 is the location of sites occupied during the NW India array vis-a-vis the position of the mapped Trans-Himalayan conductor. Figure 3 gives two sets of induction arrows corresponding to the periods of 46 and 82 min for all stations of the Garhwal and the Kangra arrays. The induction arrows for four northern-most stations of the NW India array are also included. Two distinct patterns, one corresponding to reversed arrow pattern on the eastern part

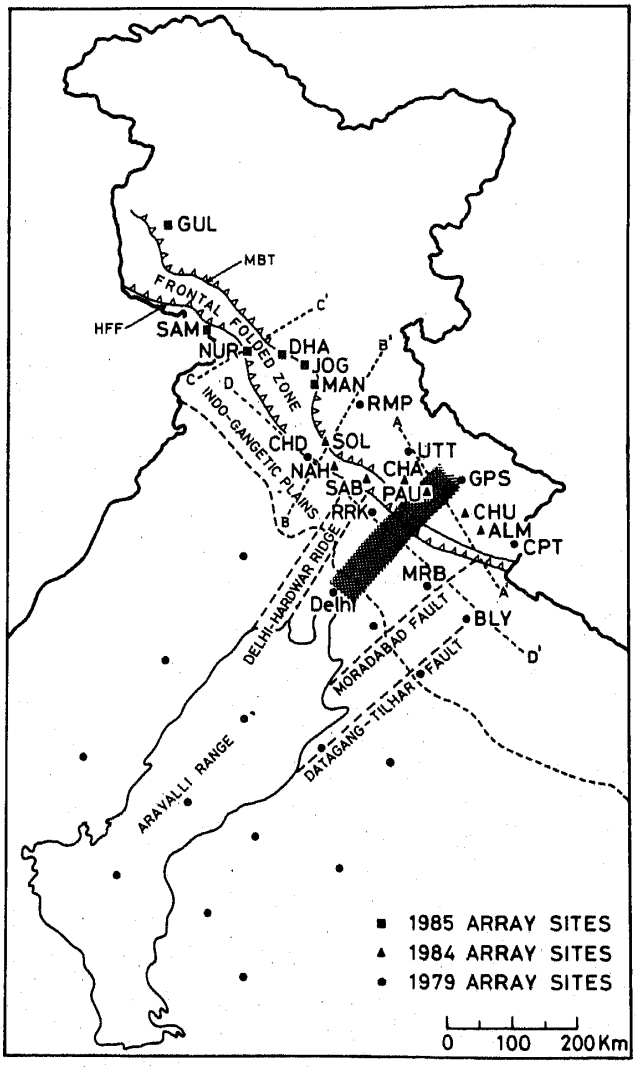

Figure 2. Map showing location of magnetometer sites occupied during 1979 (NW India), 1984 (Garhwal), 1985 (Kangra) arrays. Also shown is the position of Trans-Himalayan conductor over Ganga basin and lesser Himalaya. The lines *AA'*, *BB'*, *CC'* and *DD'* mark traverses referred to in the text.

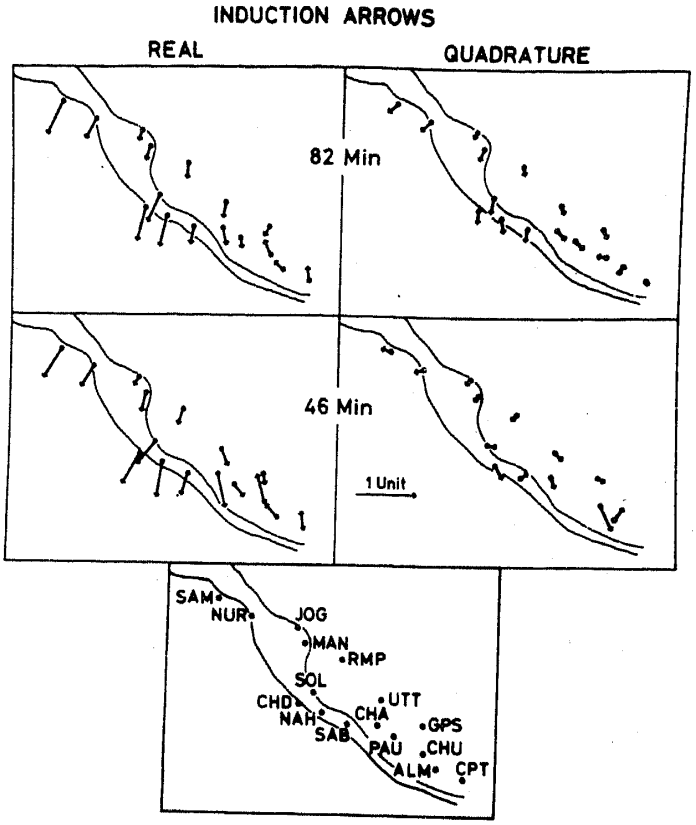

Figure 3. Real and quadrature induction arrows for periods of 82 and 46 min for the stations shown in the lower panel. Arrows point at right angles towards the region of high electrical conductivity contrast.

and the second with SSW directed arrows on the western part clearly confirm the existence of two contrasting conductive structures. The salient features which help to characterize the true nature of these induction anomalies are summarized below:

3.1 *Himalayan foothill conductivity anomaly*

At stations of the Garhwal array, away from the influence of the Trans-Himalayan conductor, as well as at all stations of the Kangra array the real induction arrows point at right angles to the Himalayan Frontal Fault (HFF) and their magnitude increases steadily as one moves from lesser Himalayan zone towards the frontal folded belt and Indo-Gangetic plains (figure 3). Examination of the anomalous vertical and horizontal fields, obtained through the HEA technique, along the two traverses *BB'* and *CC'* on figure 4 (traverse position marked on figure 2) indicates that when an incident inducing horizontal field is polarized at right-angles to the HFF, it produces a strong anomalous field whereas the orthogonal polarization induced practically no response. This polarization dependence coupled with the observation that the anomalous vertical and horizontal fields attain a maximum value close to the HFF, suggests that the anomaly can be associated with some electrical discontinuity aligned with the foothills of Himalaya.

Mahashabde *et al* (1989), while demonstrating that the spatial and polarization characteristic of the anomalous features observed across the HFF depict many features

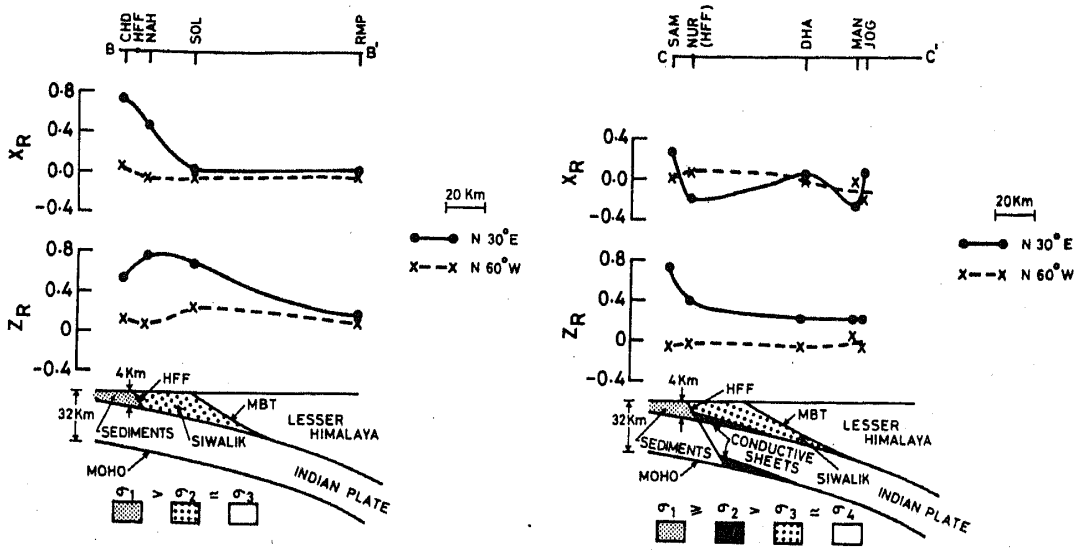

Figure 4. Spatial variation in the real part of the anomalous horizontal (X_R) and vertical (Z_R) field along the traverses (**a**) *BB'* and (**b**) *CC'* (shown in figure 2) for two polarizations of horizontal field. Lower panels give the inferred distribution of electrical conductivity in the schematic geological cross section (after Mahashabde *et al* 1989).

similar to those observed across the coastline, interpreted the induction pattern in terms of the edge effect of the sheet currents induced in the thick conducting sediments of the Indo-Gangetic plains. Further, consistent with the gravity anomalies (Lyon Caen and Molnar 1985), the sharp decay of the vertical field (Z_R) on the profile *CC'* in comparison to that along the traverse *BB'* has been interpreted to indicate the variable thrusting of sediments beneath the Siwalik and lesser Himalaya along with the subducting Indian plate. The overall signatures of the induction anomalies across the Himalayan foothills are similar to those observed along the major subduction zone. In our opinion, the water driven off the downgoing Indian plate by the dehydration process and possibly trapped in the overlying thrusted sediments provides attractive explanation for the likely seat and cause for the zone of enhanced conductivity.

3.2 *Anomalous induction and Trans-Himalayan conductor*

The reversal in the directional pattern of induction arrows on the eastern part of figure 3 marks the concentrated flow of induced currents along the NE-SW direction and forms a strong evidence for the continuation of the Trans-Himalayan conductor beneath the lesser Himalayan belt. The induction arrows with maxima at CHA and CHU with reversed direction suggest that the lateral boundaries of the conductive structure causing concentration of induced currents are located between these two stations. The polarization and frequency dependence of the anomaly, which hold information on the dimensionality and depth of mapped structure, are examined by constructing the pseudosections for various source field polarizations. Following the procedure outlined by Ingham *et al* (1983), the modulus of the vertical field responses, Z_M in equation (11), for each site at six different periods is placed and contoured on the pseudosection. Here, the horizontal scale is the distance along the traverse and vertical scale is some function which increases in value with depth into the earth

(usually the square root of the period). Figure 5 gives the pseudosection of Z_M for horizontal source field linearly polarized along $-30°$, $+60°$ (upper panel), $+30°$ and $-60°$ (lower panel) with respect to the north. On the pseudosection corresponding to the incident source field polarized at N 30°W, one finds low Z_M beneath PAU and GPS with well-developed highs on either side. The corresponding phase values, computed using equation (12), have opposite signs. The above pattern persists with reduced amplitude for fields at N 30°E and N 60°W but almost diffuses away when the incident field is polarized at N 60°E. This polarization dependence is consistent with the induction in a two-dimensional elongated conductor located beneath PAU and GPS and striking N 60°E. It is also worthy of note that induction effect is most pronounced around the period range of 40–50 min. Away from the influence of this massive structure, pseudosection shows another polarization-dependent anomaly associated with the Himalayan foothill anomaly discussed in the earlier section.

3.3 *Numerical models for the Trans-Himalayan conductor*

Three distinct two-dimensional geoelectrical models have been published to describe the basic structure of the Trans-Himalayan conductor. Numerical model studies by Vozoff (1984) to account for induction pattern over the Ganga basin (along traverse *DD'* on figure 2) suggested certain upper limits on the shape parameters of the conductive zone. He showed that the conductive zone must be 100–200 km wide, with its top surface at 10 km or less. The body was required to have resistivity less than 2 ohm.m to account for the large peak magnitude of the anomaly. Arora and Mahashabde (1987) found that the observed induction pattern for 46 min along the lesser Himalayan belt (traverse *AA'*) could be explained by asthenospheric ridge, some 45 km wide with its top at a depth of 15 km and a resistivity of 2 ohm.m. Singh and Pedersen (1988) found that the computed response reported in Arora and Mahashabde (1987) was incompatible with observations. Chamalaun *et al* (1987), approximating the anomaly response curve by recourse to the HEA technique, estimated the conductor to lie at a depth of 32 km with a width of 110 km and conductivity contrast of 1000.

Chamalaun *et al* (1987) discussed factors contributing to the non-uniqueness of the proposed model. Those limitations are equally valid for the model proposed in Arora and Mahashabde (1987). It seems that the uncertainties arising due to the large station spacing could result in a poor definition of the observed response profile which ultimately determines the model parameters and their interpretation. The control of station spacing on the resolution of the model parameters is well illustrated from the results of the Garhwal array. The inter-station spacing in the Garhwal profile was of the order of 30–50 km as against the spacing of 100–150 km in the earlier NW India array. On the Garhwal array data, the peak Z values with opposite sign at CHA and CHU, diagnostic of the likely depth a width of the involved conductor, are separated by approximately 85 km as against the estimated separation of 165 km based on the NW India array. This clearly warrants that the earlier estimates on the width of the conductor as reported in Vozoff (1984) and Chamalaun *et al* (1987), based on the data of NW India array, have been seriously constrained by the large station spacing. Furthermore, the accuracy of the computed response lies in both the function of the size and the uniformity of the grid mesh adopted in numerical modelling. It seems likely that the highly differing response obtained by Arora and

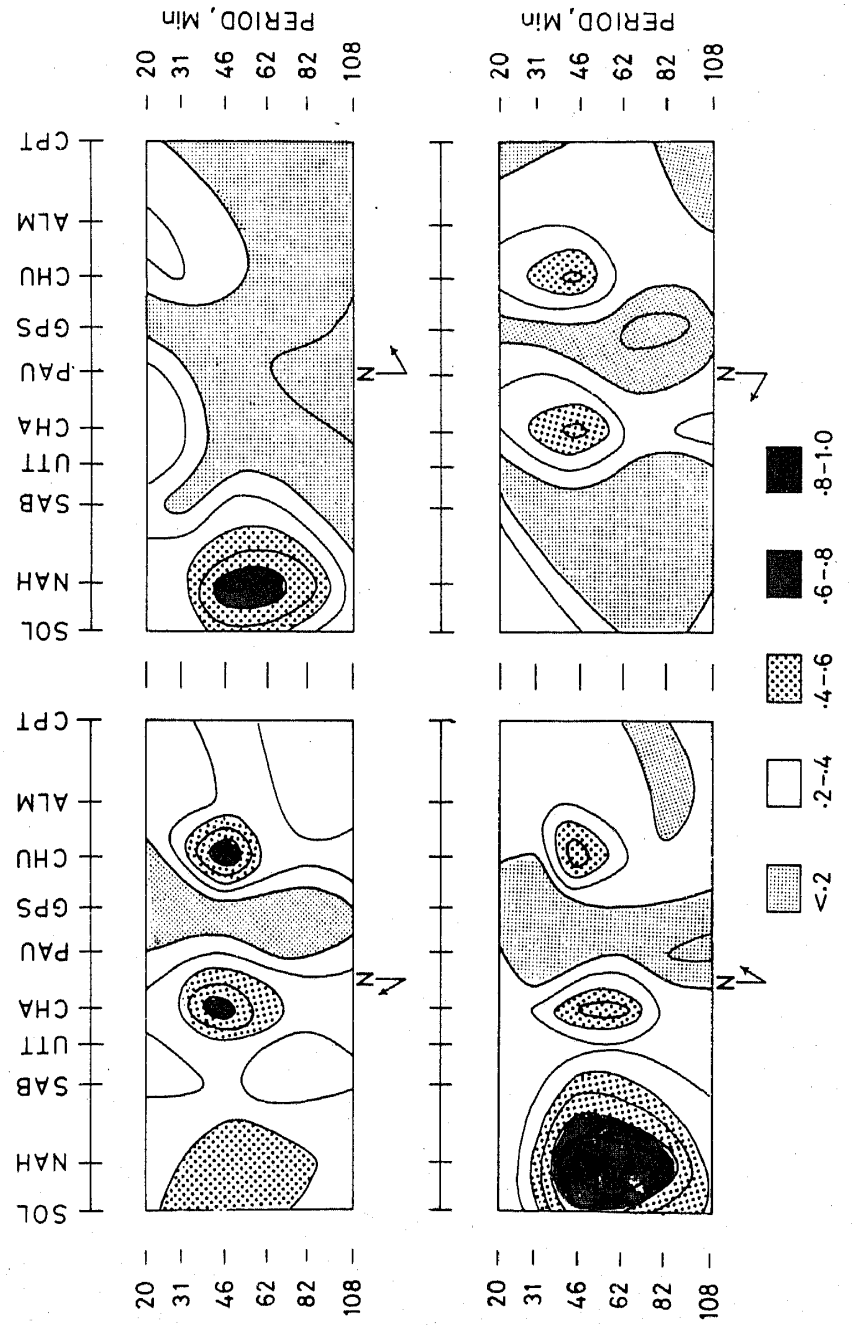

Figure 5. Pseudosection of the modulus of the anomalous vertical field (Z_M) along the 1984 profile for four polarizations of hypotheical horizontal field. The vertical scale is proportional to the square-root of period (after Arora and Mahashabde 1987).

Mahashabde (1987) and Singh and Pedersen (1988) for a given model may be the artifact of the inadequate choice of the grid dimensions. It should also be noticed that in all these exercises, the accuracy of the model is tested by comparing observed and computed response at a single frequency. More realistic constraints on the best-fitting model can be provided by comparing responses over a wide range of frequencies. Such an attempt has been more recently accomplished by Arora *et al* (1991). Demonstrating the compatibility of both the Garhwal and the NW India array data, they estimated the observed response of the conductor by combining data of both arrays along a traverse normal to the strike of the conductor. The observed response functions were computed for a polarization of horizontal field which maximizes induction effect. The reliability of the proposed geoelectrical model has been tested by comparing the observed and calculated responses at periods of 46, 67 and 82 min. The two-dimensional forward modelling approach, incorporating the numerical scheme of finite difference, developed by Brewitt-Taylor and Weaver (1976), has been used to compute the induction response of geoelectrical model. Examining a variety of models, Arora *et al* (1991) found that many of the spatial and frequency characteristic of the real part of vertical field response at three periods could be reproduced (figure 7) by induction response of two tabular blocks of 3 ohm.m shown in figure 6a. The left block is approximated to have a width of 25 km, a thickness of 12 km with its top at a depth of 8 km. The right block with its top at 12 km depth is approximated to have a width of 38 km and a thickness of 18 km. Partial modification of these block structures, as shown in figure 6a, further helps to account for the sharp gradient of the anomaly near the centre. The inclusion of a surface-conducting layer simulating conducting sediments of the Indo-Gangetic plains, with a thickness equivalent to the depth of basement along the traverse (Raiverman *et al* 1983) further improves the nature of fit for the real part of the anomaly (figure 7). The imaginary part is affected in a more pronounced manner such that the computed response tends to be much closer to the observed pattern.

The effect of the background conductivity profile on the model parameter has been invesitgated by introducing two different types of conducting layer structures at depth, as shown in figures 6b and c. Figure 6b corresponds to a well-developed electrical asthenosphere and figure 6c represents a moderate or transitional asthenosphere. This introduction of conducting layers in the background results in the attenuation of computed response. However, the changes in the model parameters to compensate for the reduction in response showed that a marginal increase in the conductivity of anomalous structure, without any significant change in the shape parameters, reproduces the observed spatial and frequency characteristics, implying that the lack of information on the true state of electrical asthenosphere has partially constrained the resistivity estimation of structure but the shape and depth parameters are fairly well determined.

A small percentage of silicate melt in interconnected spaces or the trapped hot saline water can provide resistivity of 2–3 ohm.m required to model the induction anomaly. In the absence of information on seismic velocity structure and paucity of heat flow measurements over the area of induction anomaly, it is difficult to speculate on the true mechanism for enhanced conductivity. However, the signature of certain structural discontinuity aligned with the mapped conductivity structure is well supported by the gravity map. Over the Ganga basin, conductive structure coincides with the break in isostatic gravity contours, which otherwise follow the strike of the

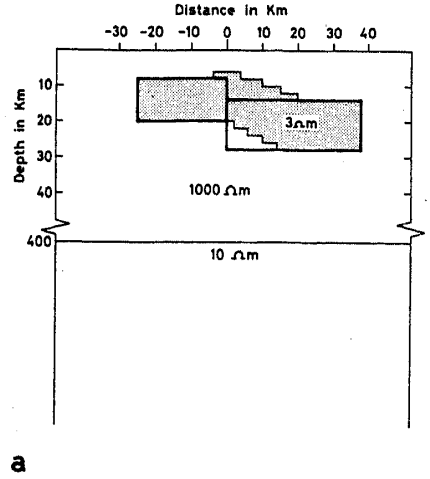

a

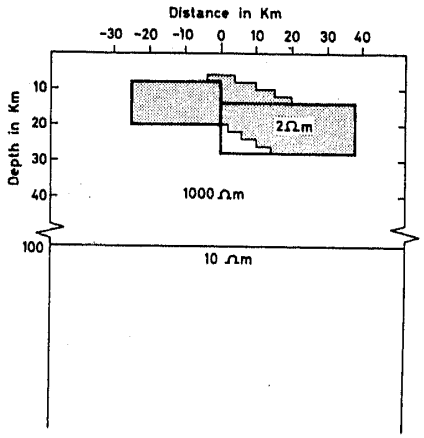

b

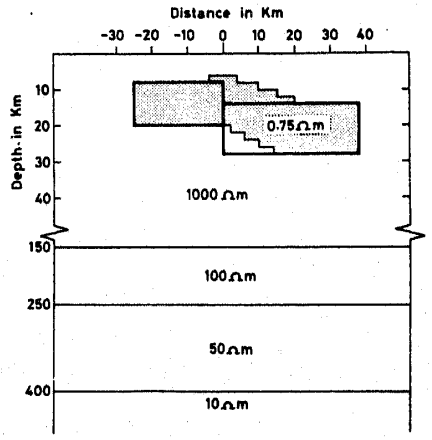

c

Figure 6. (**a**) Proposed geoelectrical model for the Trans-Himalayan conductor whose electromagnetic response is shown in figure 7. Models (**b**) and (**c**) include background conductivity distribution at greater depths representing respectively the well developed and moderate electrical asthenosphere.

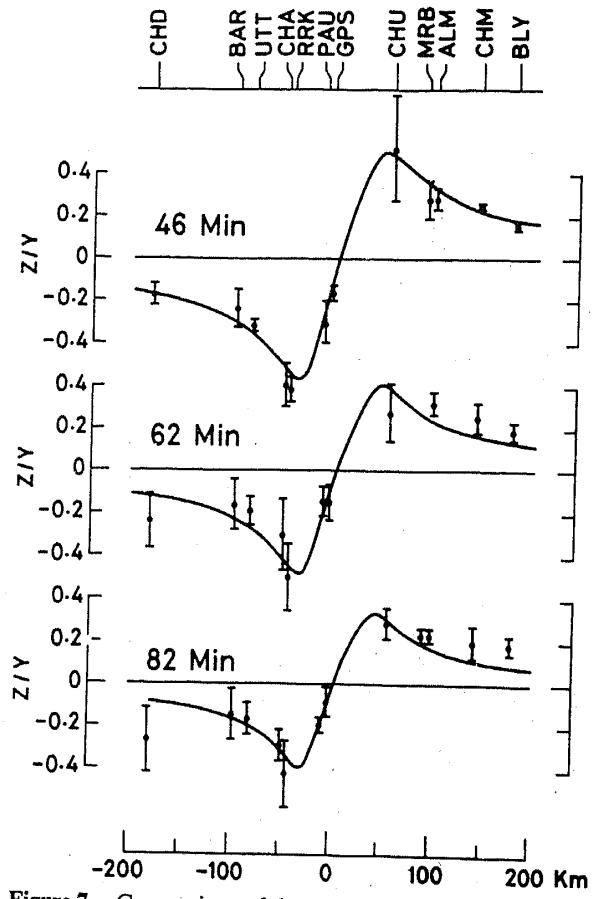

Figure 7. Comparison of the real part of the calculated vertical field for geoelectrical model shown as strippled zone in figure 6a with observed data at three periods.

Himalayan collision boundary (Qureshy 1969). Noting the alignment of mapped conductive structure with the Aravalli range, Lilley *et al* (1981) interpreted it as a continuation of the Aravalli belt being thrust down by the collision of India and Asia and made highly conductive by the conditions of stress and temperature which it is experiencing. On the quantitative seismicity map (Kaila and Narain 1976) the area of the conductivity anomaly is characterized by a transverse zone of high seismicity. This correlation suggests that the discovered conductivity may be associated with the present tectonic activity or with an ancient tectonic structure which may be reactivating.

4. Geomagnetic induction anomalies in peninsular India

The results of the array experiment in peninsular India have been dicsussed by Thakur *et al* (1981) and Srivastava *et al* (1982). The delineation of strong current concentration between India and the Sri Lanka island has been linked with the presence of a geological conductor beneath Palk Strait. In a subsequent detailed study Thakur *et al* (1986), based on the features observed on the Fourier transform contour maps along with the induction arrows, indicated a complex pattern. The anomalies were classified into four categories: (i) Southern peninsula anomaly, (ii) Pondicherry Rift

anomaly, (iii) Palk Strait anomaly, and (iv) Anomalies in the central land part. An extremely complex situation existing at the tip of the Indian Peninsula, required 3-D modelling rather than 2-D modelling.

4.1 *3-D model using finite difference approach*

Figure 8a gives the numerical model used by Ramaswamy *et al* (1985) to simulate induction anomalies of southern India. They have done the modelling excercise with or without a conductor in the Palk Strait, indicated by hatched area in figure 8a. The results were examined and compared with the observations in the form of contour plots of the amplitudes of magnetic field components. In spite of the slight discrepancy between the computed results and the observations there is an acceptable level of good fit for the model with a conductor in the Palk Strait. These discrepancies have been attributed to the crude straight line approximation in the numerical computation for the irregular coastlines of both India and Sri Lanka. Added to it, a very large area has to be incorporated into a small number of grid-cells. Though not free from limitations, a good agreement between the observed values and the numerical results for the model with a conductor is encouraging. This supports the hypothesis of sub-surface geological conductor in the channel between India and Sri Lanka island (Singh *et al* 1977; Nityananda *et al* 1977; Rajaram *et al* 1979).

4.2 *Thin-sheet model*

Following the approach of thin-sheet approximation, Mareschal *et al* (1987) modelled the magnetometer array data with special emphasis on the off-shore geology. They pointed out that the model of Ramaswamy *et al* (1985) reproduces the magnetic variations observed on the eastern coast of India quite well, but gives a trend opposite to the variations recorded along E-W profiles through the southern tip of India. In this region, the graphite occurrences are quite common. In SW Sri Lanka, the largest deposits in the world are found. Nityananda and Jayakumar (1981) pointed out that the high electrical conductivity of the mineral could definitely affect the local induction response at some stations. Srivastava *et al* (1982) identified the association of a large gravity low due to a highly resistive granitic batholith near Kodaikanal. This resistive batholith would play a role in reducing the horizontal variation component of the region while proportionally enhancing the Z component. Modelling the induction response of peninsular India is extremely difficult due to its complex tectonism and mineralization, patches of highly different conductivities on land and also due to the presence of the sea. Only limited success in modelling could be attained in such situations, since a unique definition of the geological situation is not possible. In the model described by Mareschal *et al* (1987) particular emphasis has been on the geological characteristics of the regions directly off the coast of India. Besides the limitations of the thin-sheet approximation that it breaks down above a certain frequency range, another drawback is that it artificially confines all heterogeneities to a thin layer. The thickness (or thinness) is so chosen that at a given period the horizontal electric field is constant from surface to the bottom of each of its individual cells. As is true of any numerical method, the thin-sheet approximation is also limited by the number of cells that can be included in the model.

In order to test whether a single conductor located in the Indo-Ceylon graben,

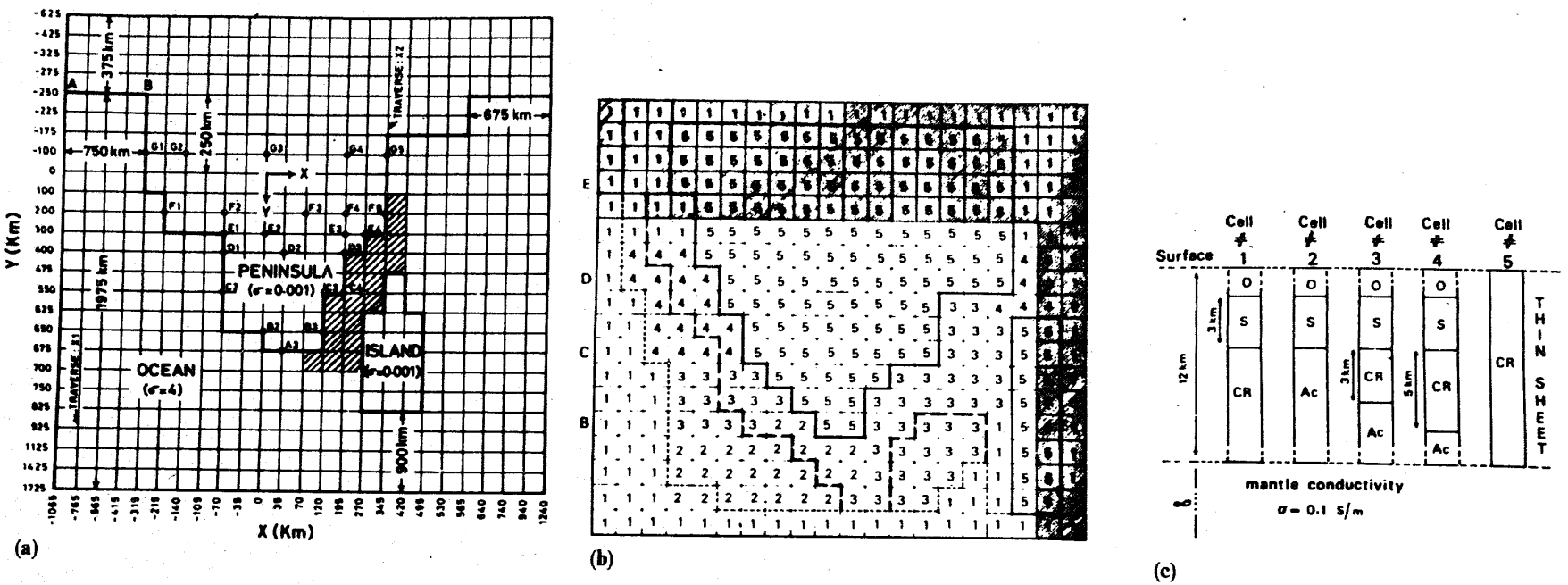

Figure 8. (**a**) Numerical model on the x-y plane at the surface $z = 0$. The hatched area is the surface projection of the buried conducting structure (denotes conductivity values in $S\,m^{-1}$) (after Ramaswamy *et al* 1985). (**b**) Horizontal section: the dashed line follows the 200 m isobath, the dotted line follows the 1000 m isobath. The five basic cells have 'equivalent conductivities' corresponding to the vertical pseudosections given in (**c**) ($\sigma(0) = 4\,S\,m^{-1}$; $\sigma(S) = 1\,S\,m^{-1}$; $\sigma(Cr) = 0{\cdot}001\,S\,m^{-1}$; $\sigma(Ac) = 1\,S\,m^{-1}$). The exact conductivity for a given cell (execpt for cells '5' which represent the land) depends on the thickness of water selected as top layer (200, 1000 or 2000 m, see isobaths in (**c**) I (after Mareschal *et al*) 1987).

could satisfy the data base, a model of the peninsular India was constructed in the presence of the surrounding seas and induction arrows generated at 108 min. The resulting model induction vectors, when compared with those that were reduced from the data base, did not compare well. This led Mareschal *et al* (1987) to look for some other explanation. The schematic model (figure 8b) considered included a crustal conductor under the Comorin ridge or its proximity and may be related to the uprising of the mantle material or to mineralizations. A second conductor has been placed in the Indo-Ceylon graben which has an integrated conductivity slightly inferior to that of the region south of Trivandrum. Though not free from limitations, this model seems to follow the observations better than the model based on a single conductor underneath the Palk Strait. Mareschal *et al* (1987) argued that the two conductors proposed in their model studies might be connected through the development of rift system associated with the break-up of Gondwanaland, and the conductor south of Trivandrum possibly corresponding to some kind of Triple junction between the Comorin ridge, Indo-Ceylon graben and west coast rifting. The numerical model on this line bas been further refined by Agarwal and Weaver (1989). The tectonic implications of this model are discussed separately in this issue.

In both the 3-D and thin sheet modelling exercises, the background conductivity at depth, simulating electrical asthenosphere, has been approximated by half-space of 10 ohm.m extending from a depth of 30 km. Long-period magnetotelluric investigations have shown the depth to the electrical asthenosphere in tectonically active and stable shield region to be located around 100 and 400 km respectively (Vanyan 1981). As seen with the numerical model excerise for the Trans-Himalayan conductor the computed induction response for envisaged anomalous structure gets attenuated by the inclusion of conducting layer in the background layered medium and it seems plausible that the very high conductivity values which were required to be assigned to various anomalous structures to reproduce response with magnitude comparable to observed strength may be an artifact of including highly conducting asthenosphere at a shallow depth of 30 km. It should be noted that neither Ramaswamy *et al* (1985) nor Mareschal *et al* (1987) considered any heterogeneity on the land. Inclusion of such effects, consistent with other geophysical data, would be further helpful in the geological interpretation of mapped structure.

5. Geoelectrical structures associated with a seismically active zone of Valsad

The mini-magnetometer array study over the Deccan trap-covered region of western India was designed to probe the structural configuration of a localized seismic zone in district Valsad, south Gujarat, which is experiencing a swarm of seismic activity since early 1986. The results of this array have been recently compiled by Arora and Reddy (1990). Figure 9a gives the location of study area in relation to various tectonic elements of the western India. The layout of the magnetometer sites in relation to the concentrated belt of earthquake epicentre is shown in figure 9b. Figure 10a gives a typical example of the nature of transient variation recorded by the array. The most conspicuous feature of the transient variations is the anomalous enhancement of Y component, unaccompanied by any significant anomaly in X and Z components, at stations bounding the seismically active area. This anomalous behaviour of Y-component becomes much more apparent in the plot of anomalous

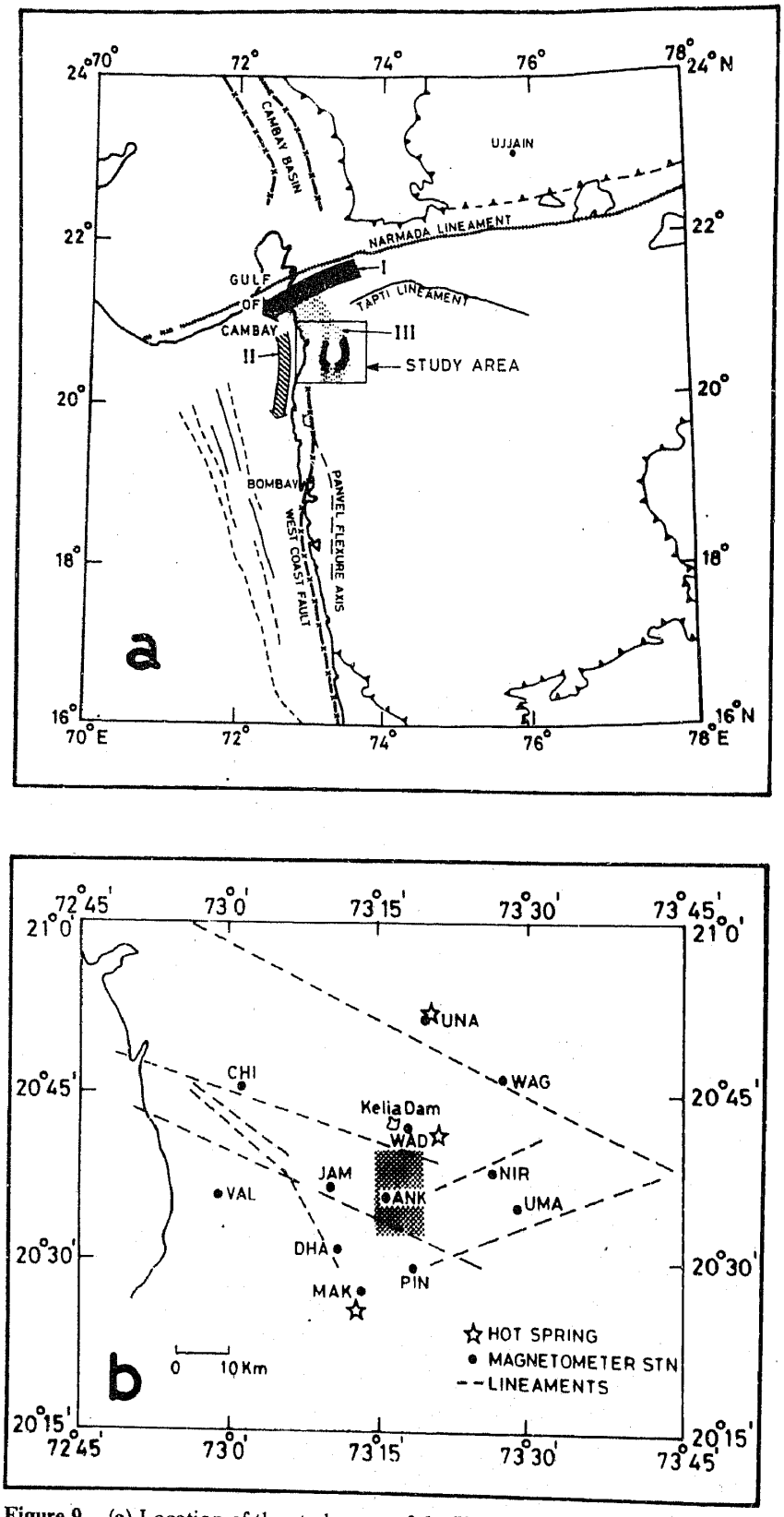

Figure 9. (a) Location of the study area of the Valsad magnetometer array on the tectonic map of western India, together with the inferred flow path of concentrated internal induced currents. (b) Layout of the magnetometer sites in the study area in relation to the presently active seismic (hatched area) zone.

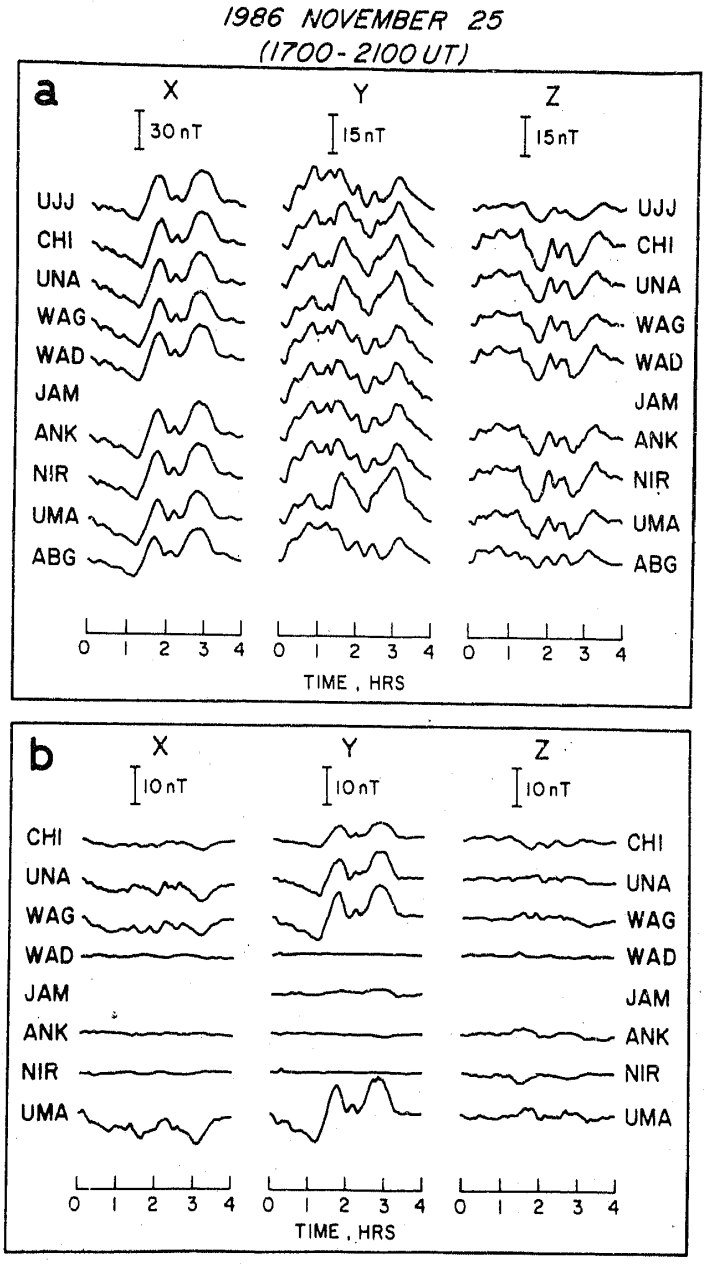

Figure 10. (a) Stacked plots of magnetovariational event for 8 stations of the Valsad array and for two regular observatories; (b) Anomalous field variation corresponding to the event shown in the upper panel.

field (figure 10b), obtained by subtracting the field variations corresponding to the average pattern of the central group of stations which on comparison with the records of distant magnetic observatories Alibag (ABG) and Ujjain (UJJ) were found to represent a uniform normal field. This anomalous behaviour was taken to indicate that the central part of the array, roughly defined by the concentrated belt of the earthquake epicentres, denotes a resistive block embedded in an approximately north-south oriented conductive belt. This inference is further corroborated by the various analysis techniques to which data were subjected. Figure 11 gives a set of induction arrows, perturbation arrows and anomalous induction arrows as defined

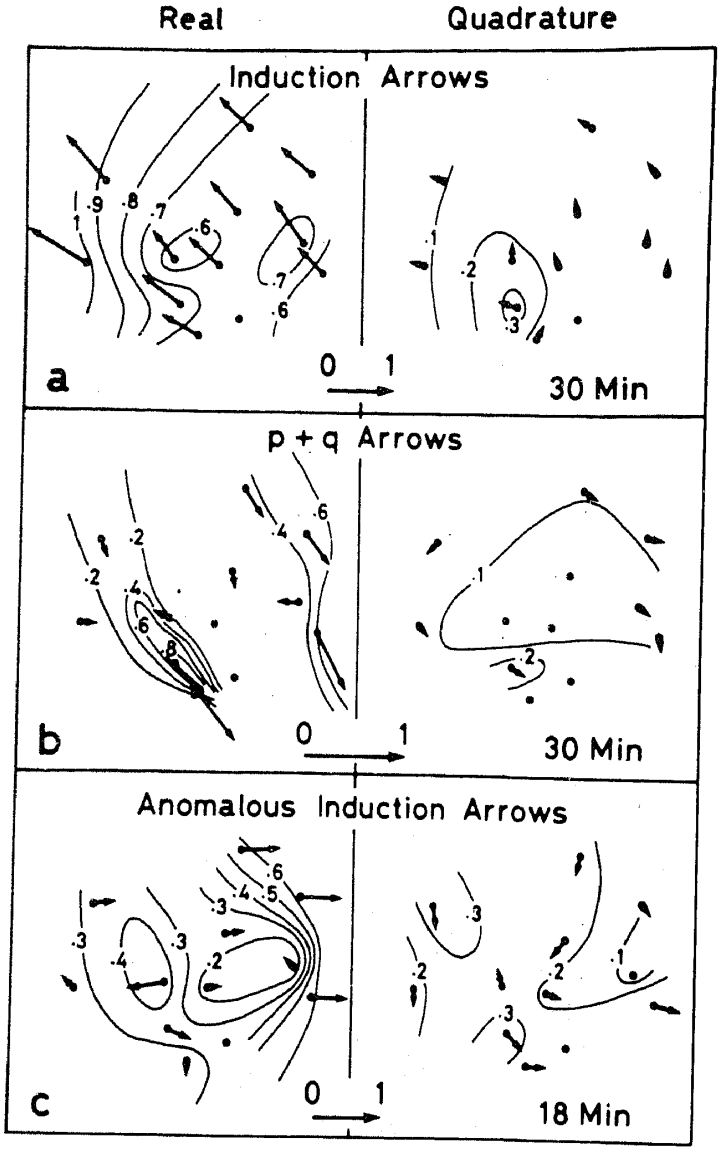

Figure 11. Real and quadrature (**a**) induction, (**b**) combined $p+q$ and (**c**) anomalous induction arrows. Magnitude contour plots are also shown.

in §2. The various anomalies noted on these different modes of data presentation indicate the existence of a complex induction pattern controlled by a combination of conductive and resistive structures related with larger tectonic features of the region. The overall inferred flow pattern of internal induced currents compatible with various anomalous effects is superimposed in figure 9a. The real induction arrow with consistent northwesterly orientation at all stations clearly indicates the presence of a high conductivity zone along segment I of the flow path of internal current. In conjunction with the gravity, magnetization pattern and high thermal anomaly, the presence of a high conductivity zone to the northwest array supports the hypothesis of a plume-associated triple junction beneath the Gulf of Cambay (Biswas 1987). The current segment II on figure 9a, flowing parallel to the western continental margin is consistent with the concentration of induced currents in conducting sea water, and may account for the enhancement of Z at coastal stations CHI and VAL.

The physical evidence resulting from the interpretation of $\mathbf{p}+\mathbf{q}$ arrows that the anomalous internal current entering the array from north are predominantly directed along the NNW-SSE, is taken to indicate an electrical conductive structure aligned with segment III of the current path in figure 9a. The observational evidence that the anomalous Y variation in time domain (figure 10b) varies almost in-phase with the normal X variations (figure 10a) further suggests that the generating mechanism for anomalous flow along structure III is more likely to be associated with the channelling of currents initially flowing in the east-west direction. The prevailing high heat flow values and the physical evidence from the deep seismic work that the west coast of India in the vicinity of present study area represents a region of Moho upwarp (Kaila 1986) suggests that the upwarped asthenosphere along segment III may act as a conducting path to channel induced currents out of the region of the Cambay triple junction. The flow path of anomalous internal currents along segment III becomes quite intricate near the seismically active zone which is identified as resistive block embedded in conductive environment. In such a configuration, the channelled currents from north due to obstruction by a highly resistive block will be deflected into two narrow channels on either side of the resistive block. Because of the conservation of currents, the current density in the conducting host will be appreciably enhanced leading to the enhancement of the Y component, as observed. Such geometrical configuration would also produce a large spatial gradient in the vertical field as clearly borne out on the map of the anomalous induction arrow (figure 11c). Consistent with an evolutionary model of the Deccan volcanism, it is visualized that the central resistive block coincident with the concentrated belt of earthquake epicentres represents a plutonic body embedded in conducting upwarped mantle/asthenosphere. Magneto-telluric studies initiated recently confirm the existence of a large resistivity contrast between the seismically active zone and just outside. A 2-D modelling of this and fresh magnetotelluric data would provide better constraints on the geological interpretation of the mapped structure.

6. Concluding remarks

Magnetometer array studies carried out so far in India have established their utility, atleast as an effective reconnaissance survey tool, to provide information on the deep structures in terms of electrical conductivity distribution. The mapped Trans-Himalayan conductor is essentially one of the largest and most significant continental geomagnetic induction anomalies. Modelling gives more definite insight into the source mechanism, on other geometrical configuration of the mapped conductive body, but its validity should only be reckoned in the light of the quality of the data base and the constraints imposed on the modelling exercise. With the availability of real quality data base, both from the viewpoint of station-spacing and frequency content, more comprehensive modelling enabled one to define the true geometrical parameters of the Trans-Himalayan conductor. As the induction effect over the Ganga basin is found to be complex and changes over short distances, 3-D modelling may be desirable to clarify the influence of induction taking place in sediments. Incorporation of a realistic background conductivity depth profile from long-period magnetotelluric survey will further help to quntify the true conductivity contrast of the mapped anomalous structure.

The nature of the induction effects both in the southern peninsula and near the western continental margin emphasizes the need for simultaneous measurements on the ocean floor. With the availability of the ocean bottom magnetometers at IIG, such surveys could now be undertaken. Inputs from such measurements will put suitable restraint on the range of models for the southern peninsula. It will be worthwhile mentioning that no forward modelling solution can be unique in all respects. At this stage integration of geoelectrical models with other geophysical inputs such as gravity, magnetic, seismic wave velocities and heat flow etc can provide important clues to identify the mechanism that causes the anomalies and in bringing out the correct geological picture.

Acknowledgements

The author is extremely grateful to Professor B P Singh for his role in launching the magnetometer array work in India. Expertise and help received from Dr F E M Lilley during the early years of array work in India is gratefully acknowledged. The author also wishes to thank Dr S N Prasad for many fruitful discussions and exchange of ideas through correspondance. Financial support received from the Department of Science and Technology, New Delhi for investigating the conductivity anomalies in different parts of India is acknowledged with thanks.

References

Adam A 1980 The change of electrical structure between an orogentic and the ancient tectonic area (Carpathians and Russian plateform); *J. Geomagn. Geoelectr.* **32** 1–46

Agarwal A K and Weaver J T 1989 Regional electromagnetic induction around the Indian peninsular and Sri Lanka; a three dimensional numerical model study using the thin sheet approximation; *Phys. Earth Planet. Inter.* **54** 320–331

Alabi A O 1983 Magnetometer Array Studies; *Geophys. Surv.* **6** 153–172

Arora B R 1987 Perturbation arrows and hypothetical event analysis in geomagnetic induction studies: experimental results from northwest India; *Phys. Earth Planet. Inter.* **45** 128–136

Arora B R 1988 Electrical conductivity configuration of plate collision boundary of northwest India; *Proc. Sixth Indian Geol. Cong.* (ed) P S Moharir, (Univ of Roorkee) pp. 47–52

Arora B R, Kaikkonen P and Mahashabde M V 1991 The numerical model and tectonic implications of the Trans-Himalayan conductor of NW India (under preparation)

Arora B R, Lilley F E M, Sloane M N, Singh B P, Srivastava B J and Prasad S N 1982 Geomagnetic induction and conductive structures in northwest India; *Geophys. J. R. Astron. Soc.* **69** 459–475

Arora B R and Mahashabde M V 1987 A transverse conductive structures in the northwest Himalaya; *Phys. Earth Planet. Inter.* **45** 119–127

Arora B R and Reddy C D 1990 Magnetovariational study over a seismacally active area in Deccan Trap of western India; *Phys. Earth Planet. Inter.* (in press)

Bailey R C, Edwards R N, Garland G D, Kutz R and Pitcher D 1974 Electrical conductivity studies over a tectonically active area in eastern Canada; *J. Geomagn. Geoelectr.* **26** 125–146

Beamish D 1977 The mapping of induced currents around the Kenya rift: a comparision of techniques; *Geophys. J. R. Astron. Soc.* **50** 311–332

Biswas S K 1987 Regional tectonic framework, structure evolution of the western marginal basins of India; *Tectonophysics* **135** 307–327

Brewitt Taylor C R and Weaver J T 1976 On the finite difference solution of two-dimensional induction problems; *Geophys. J. R. Astron. Soc.* **47** 375–396

Chamalaun F H, Prasad S N, Lilley F E M, Srivastava B J, Singh B P and Arora B R 1987 On the

interpretation of the distinctive pattern of geomagnetic induction observed in northwest India; *Tectonophysics* **140** 247–255

Gough D I 1983 Electromagnetic geophysics and global tectonics; *J. Geophys. Res.* **88** 3367–3377

Gough D I and de Beer J H 1980 Conductive structures in southernmost Africa: a magnetometer array study; *Geophys. J. R. Astron. Soc.* **63** 479–495

Gough D I and Ingham M R 1983 Interpretation methods for magnetometer arrays; *Rev. Geophys.* **21** 805–827

Hjelt S E 1988 Regional EM studies in the 80's; *Surv. Geophys.* **9** 349–387

Hutton R 1976 Induction studies in the rifts and other active region; *Acta Geod. Geophys. Montan* **11** 347–376

Ingham M R, Bingham D K and Gough D I 1983 A magnetovariational study of a geothermal anomaly; *Geophys. J. R. Astron. Soc.* **72** 597–618

Jones A G 1983 The problem of current channelling: a critical review; *Geophys. Surv.* **6** 79–122

Jones A G 1986 Parkinson's pointers' potentail perfidy; *Geophys. J. R. Astron. Soc.* **87** 1215–1224

Jones F W and Pascoe L J 1971 A general computer program to determine the perturbation of alternating electric currents in a two-dimensional model of a region of uniform conductivity with an embedded inhomogeneity; *Geophys. J. R. Astron. Soc.* **24** 3–30

Kaikkonen P 1986 Numerical electromagnetic modelling including studies of characteristic dimension: A review; *Surv. Geophys.* **8** 301–337

Kaila K L 1986 Tectonic framework of Narmada-Son lineament – A continental rift system in central India, from deep seismic soundings In: *Reflection seismology: A global prospective* (eds) M Barazangi and L Brown (Geodynamic Series AGU Publ.) **13** 133–150

Kaila K L and Narian H 1976 Evolution of the Himalaya Based on seismotectonics and deep seismic soundings: *Proc. Himalyan Geology Seminar, Section 11-B: structures, Tectonics,* Seismicity and Evolution pp. 1–30

Lilley F E M, Singh B P, Arora B R, Srivastava B J, Prasad S N and Sloane M N 1981 A magnetometer array study in northwest India: *Phys. Earth Planet. Inter.* **25** 232–240

Lyon-Caen H and Molnar P 1985 Gravity anomalies, flexure of the Indian plate and the structure, support and evolution of the Himalaya and Ganga basin; *Tectonics* **4** 513–538

Mahashabde M V, Waghmare S Y and Arora B R 1989 Anomalous geomagnetic variations and possible causative structures along foothills of Himachal Pradesh-Kumaun-Himalaya; *Proc. Indian Acad. Sci. (Earth Planet. Sci.)* **98** 319–326

Mareschal M, Vesseur G, Srivastava B J and Singh R N 1987 Induction models of southern India and the effect of offshore geology; *Phys. Earth Planet. Inter.* **45** 137–148

Nityananda N, Agarwal A K and Singh B P 1977 Induction at short period on the horizontal field variation in the Indian Peninsula; *Phys. Earth Planet. Inter.* **15** 5–9

Nityananda N and Jayakumar D 1981 Proposed relation between anomalous geomagnetic variations and the tectonic history of south of India; *Phys. Earth Planet. Inter.* **27** 223–228

Raiverman V, Kunte S V and Mukherjee A 1983 Basin geometry, Cenozonic sedimentation and hydrocarbon prospects in north western Himalaya and Indo-Gangetic Plains, Petroliferous basins of India, Himachal Times Group, Dehradun 67–92

Rajaram M, Singh B P, Nityananda N and Agarwal A K 1979 Effect of the presence of a conducting channel between India and Sri Lanka on the features of the Equatorial Electrojet; *Geophys. J. R. Astron. Soc.* **56** 127–138

Ramaswamy V, Agarwal A K and Singh B P 1985 A three-dimensional numerical model study of the electromagnetic induction around the Indian peninsula and Sri Lanka island; *Phys. Earth Planet. Inter.* **39** 52–61

Reitzel J S, Gough D I, Porath H and Anderson C W 1970 Geomagnetic deep sounding and upper mantle structure in the western United States; *Geophys. J. R. Astron. Soc.* **19** 213–235

Qureshy M N 1969 Thickening of a basalt layer as a possible cause for the uplift of the Himalayas—a suggestion based on gravity data; *Tectonophysics* **7** 137–157

Schmucker U 1970 Anomalies of geomagnetic variations in the southwestern United States; *Bull. Scripps Inst. Oceanogr.* **13** 1–165

Singh B P 1980 Geomagnetic sounding of conductivity anomalies in the lower crust and upper most mantle; *Geophys. Surv.* **4** 71–87

Singh B P, Nityananda N and Agarwal A K 1977 Induced magnetic variations in the Indian peninsula; *Acta Geodact. Geophys. Montan* **12** 65–72

Singh Ramesh P and Pedersen L B 1988 A transverse conductive structure in the northwest Himalaya by B R Arora and M V Mahashabde; *Phys. Earth Planet. Inter.* **53** 177–179

Srivastava B J, Prasad S N, Singh B P, Arora B R, Thakur N K and Mahashabde M V 1982 Induction anomalies in geomagnetic Sq in peninsular India; *Geophys. Res. Lett.* **9** 1135–1138

Thakur N K; Mahashabde M V, Arora B R, Singh B P, Srivastava B J and Prasad S N 1981 Anomalies in geomagnetic variations on peninsular India near Palk Strait; *Geophys. Res. Lett.* **8** 947–950

Thakur N K, Mahashabde M V, Arora B R, Singh B P, Srivastava B J and Prasad S N 1986 Geomagnetic variation anomalies in peninsular India; *Geophys. J . R. Astron. Soc.* **86** 839–854

Vanyan L L 1981 Deep geoelectric methods: geological and electromagnetic principles: *Phys. Earth Planet. Inter.* **25** 273–279

Vozoff K 1984 Model study for the proposed magnetotelluric (MT) traverse in north India; *Tectonophysics* **105** 399–411